THE AMERICAN MINERALOGIST, VOL. 55, JANUARY-FEBRUARY, 1970

CRYSTAL CHEMISTRY OF THE BASIC IRON PHOSPHATES

PAUL B. MOORE, *The Department of the Geophysical Sciences, The University of Chicago, Chicago, Illinois, 60637.*

ABSTRACT

A general structural principle is widespread among the basic phosphates of ferrous and ferric iron. It is based on a highly stable polyatomic complex involving ferrous-ferric oxy-hydroxy octahedral face-sharing triplets. The orientation of the associated corner-linked nearest neighbor octahedra and tetrahedra is so similar in several mineral structures that a general hierarchy of structure types has been derived. Crystal structures of the various members are dictated by the ways in which the fundamental polyatomic octahedral three-cluster and its nearest neighborhood of octahedra link along a third "variable" axis.

The refined crystal structures of dufrenite and rockbridgeite are revealed. Structure cell and indexed powder data are presented for dufrenite, souzalite, rockbridgeite, beraunite, laubmannite, and mineral A (a new species). Data in the literature are misleading and largely in error for most of these compounds. Members of the basic ferrous-ferric phosphate family known to possess the octahedral face-sharing three-cluster include barbosalite, lipscombite, dufrenite, souzalite, rockbridgeite, beraunite, laubmannite, and mineral A. Other compounds which may also involve the three-cluster include azovskite, cacoxenite, richellite, mitridatite, eguëite, tinticite, borickyite, and foucherite.

All basic ferrous-ferric phosphates which possess the three-cluster are strongly pleochroic and greenish-black in color. Their completely oxidized equivalents are yellow to reddish-brown and weakly pleochroic. The relative absorption of polarized white light appears to be dictated in a complex way by the orientation of the three-cluster in the crystal, the extreme pleochroism resulting from directed charge transfer $Fe^{2+}+Fe^{3+}\rightleftharpoons Fe^{3+}+Fe^{2+}$.

Paragenetic schemes involving some of these minerals are proposed on the basis of specimen study and crystal chemistry. Typical sequences involve denser phases followed by higher hydrates. Typical steps in the hydrothermal reworking of the early phosphates involve *laubmannite→dufrenite→beraunite; rockbridgeite→beraunite; rockbridgeite→mineral A*. Color banding along the fibers in mammillary aggregates of some rockbridgeites results from the appearance of different phases. Typical species and their colors are: rockbridgeite (greenish-black), lipscombite (bluish-green granular), mineral A (brown to greenish-yellow), and beraunite (orange).

INTRODUCTION

The basic phosphates of the transition metal ions (in particular those of Fe^{2+}, Fe^{3+}, Mn^{2+}, and Mn^{3+}) are among the most perplexing substances in the mineral kingdom. Many scientists have contributed to the subject yet many species still remain insufficiently characterized. The problem is complicated, since variable oxidation states of the metals may occur for the same species. Furthermore, their frequently fibrous habit allows variable water content and nonessential impurities; their chemical compositions are often so similar that diagnostic features, such as hardness, density, color and optical properties overlap. The problem has even persisted throughout the course of early to recent X-ray diffraction studies,

and for simple reasons: many species are fibrous so that suitable single crystals are difficult to obtain and perfect cleavage directions contribute toward preferred orientation in cylindrical and slide powder mounts.

A detailed paper by Frondel (1949) serves adequately to outline the tumultuous history in this research. That paper also offers considerable insight into the problem and the crystallochemical arguments therein are quite noteworthy, especially in light of the paucity of crystal cell data available at that time. Unfortunately, the most important diagnostic properties—the X-ray powder patterns—are misleading and reference to them should be abandoned.

Additional light was shed by a paper on Fe-Mn orthophosphate hydrate classification by Moore (1965a). This paper considered these and related compounds as coordination complexes and focused attention on the importance of the octahedral clusters which were treated as polyatomic complexes in these structures. Advances in the crystal chemistry of these compounds then proceeded in normal fashion, through the systematic analysis of their crystal structures. A preliminary account of this present study appeared in Moore (1969).

The list of basic iron phosphates (Table 1) is very extensive, comprising no less than 40 species. Single hand specimens may show as many as a dozen species in close association, especially if the material was derived from hydrothermally reworked triphylite-lithiophilite. As many as 30 species are known from the reworked triphylite pods at the Palermo No. 1 Pegmatite, North Groton, New Hampshire; a remarkable collection of thousands of Palermo specimens, assembled by the late Mr. G. Bjareby and presently owned by Prof. J. V. Smith, offers a unique opportunity for detailed study of their relationships.

Two other noteworthy kinds of basic iron phosphate occurrences includes druses, knobs and bands in gossans, "limonite" and novaculite beds; and iron-rich nodules in marls, sands, and soils. The former are derived from phosphatic solutions which reworked the ferric oxy-hydroxides, and the latter are usually associated with organic remains.

The species discussed in detail in this paper include dufrenite, souzalite, rockbridgeite, laubmannite, beraunite, cacoxenite, mineral A, lipscombite, and barbosalite. Since the subject matter is rather involved and interdependent, the relevant species are briefly discussed individually, but their relationship to the general family of basic iron phosphates is given especial emphasis under the general headings. Much of this work was inspired by the formal solution of the atomic arrangements of dufrenite and rockbridgeite; these crystal structures are discussed in detail.

TABLE 1. COLORS OF THE IRON PHOSPHATE HYDRATES AND RELATED COMPOUNDS

		Color			Color
Ferrous			**Ferric**		
triphylite	$LiFe(PO_4)$	pale greenish-gray	heterosite	$Fe(PO_4)$	purple
sarcopside	$Fe_3(PO_4)_2$	pink	tavorite	$LiFe(OH)(PO_4)$	chartreuse
arrojadite	$Na_2Fe_5(PO_4)_4$	bottle-green	carminite	$PbFe_2(OH)_2(AsO_4)_2$	red
wolfeite	$Fe_2(OH)(PO_4)$	orange	dussertite	$BaFe_3(OH)_5(H_2O)(AsO_4)_2$	green
phosphoferrite	$Fe_3(H_2O)_3(PO_4)_2$	pale green	chenevixite	$Cu_2Fe_2(OH)_4(H_2O)(AsO_4)_2$	green
ludlamite	$Fe_3(H_2O)_4(PO_4)_2$	pale-green	metastrengite	$Fe(H_2O)_2(PO_4)$	pink
vivianite	$Fe_3(H_2O)_8(PO_4)_2$	colorless to blue (some Fe^{3+})	strengite	$Fe(H_2O)_2(PO_4)$	pink
			laueite	$MnFe_2(OH)_2(H_2O)_6(PO_4)_2 \cdot 2H_2O$	orange
			stewartite	$MnFe_2(OH)_2(H_2O)_6(PO_4)_2 \cdot 2H_2O$	yellow
			strunzite	$MnFe_2(OH)_2(H_2O)_6(PO_4)_2 \cdot 2H_2O$	yellow
			[a]?cacoxenite	$Fe_9(OH)_{15}(H_2O)_3(PO_4)_4 \cdot 15H_2O$	yellow
			pharmacosiderite	$KFe_4(OH)_4(AsO_4)_3 \cdot 6H_2O$	pale green
			kruzhanovskite	$MnFe_2(OH)_2(H_2O)(PO_4)_2$	greenish-brown
			[a] mineral A	?	brownish-yellow
			tinticite	$Fe_3(OH)_3(PO_4)_2 \cdot 3H_2O$	pale yellow-green
			azovskite	$Fe_3(OH)_3(PO_4)_2 \cdot 3H_2O$?	reddish
			mitridatite	$CaFe_2(OH)_2(PO_4)_2 \cdot nH_2O$	green
			diadochite	$Fe_2(OH)(PO_4)(SO_4) \cdot 5H_2O$	deep red
			equëiite	$CaFe_{14}(OH)_{14}(PO_4)_{10} \cdot 21H_2O$?	brownish-yellow
			richellite	$Ca_3Fe_{10}(OH)_{12}(PO_4)_8 \cdot nH_2O$	reddish-brown
			borickyite	$CaFe_5(OH)_{11}(PO_4)_2 \cdot 3H_2O$	brown
			foucherite	$CaFe_3(OH)_3(PO_4)_2 \cdot 7H_2O$	brown
Ferrous-Ferric					
[a]barbosalite	$Fe^{2+}Fe_2^{3+}(OH)_2(PO_4)_2$	greenish-black			
[a] lipscombite	$Fe^{2+}Fe_2^{3+}(OH)_2(PO_4)_2$	greenish-black →			greenish-yellow
[a] dufrenite	$CaFe_5^{2+}Fe_{10}^{3+}(OH)_{13}(H_2O)_4(PO_4)_8$	deep green →			brown
[a] laubmannite	$Fe_2^{2+}Fe_5^{3+}(OH)_{12}(PO_4)_4$	deep green →			tan
[a] rockbridgeite	$Fe^{2+}Fe_4^{3+}(OH)_5(PO_4)_3$	greenish-black →			brown
[a] beraunite	$Fe^{2+}Fe_5^{3+}(OH)_5(H_2O)_4(PO_4)_4 \cdot 2H_2O$	bluish-black →			reddish-orange
[a] souzalite	$(Mg, Fe)_3^{2+}(Al, Fe)_4^{3+}(OH)_6(PO_4)_4 \cdot 2H_2O$	green			

[a] Contain the *h*-cluster.

Experimental Procedure

Crystal Cell Data. Single crystals of most basic iron phosphates are very infrequently encountered, since the species usually occur as fibrous aggregates. The crystals, when they do occur, are small and curved; larger crystals are usually bunched or crinkled, prohibiting unambiguous interpretation of the complex single crystal photographs. The crystal cell data in Table 2 were obtained by splitting fibers in acetone until an optically single platelet was found. It was observed that single individuals are clear and transparent but crystal fragments, though seemingly single in outward appearance, always proved to be multiplets whenever they were turbid in reflected light, the turbidity arising from random rotations about the fiber axis.

The dufrenite (Univ. of Chicago No. 1247) used in this study occurs as greenish-black tabular crystals up to 1 mm across, superficially altered to brown oxy-hydroxides and associated with pharmacosiderite in a fractured quartz vein from Cornwall, England. The material apparently corresponds to the Wheal Phoenix specimens described by Frondel (1949). Rotation photographs about [010] and Weissenberg photographs of the 0-, 1-, and 2-levels were obtained. This same crystal was used in the three-dimensional crystal structure analysis discussed further on.

The cell data of Cornish dufrenite are similar to those reported by Mrose (1955); indeed, reorienting to the *I*-cell shows the relationship (Table 2). Unfortunately, the space group criteria are in conflict, resulting either from a misinterpretation in the earlier report or from the unlikely existence of a different but related phase. Three-dimensional crystal structure analysis confirms the space group $C2/c$ for the dufrenite from Cornwall.

The rockbridgeite crystal (Univ. of Chicago No. 799) was obtained as a splinter from Irish Creek, Virginia material. It is greenish-black in color; although the crystal was small (about 80 microns in mean dimension), it afforded superior photographs. This crystal was also used for three-dimensional crystal structure analysis, discussed further on. Inspection of an assortment of rotation and Weissenberg photographs led to the cell criteria in Table 2. The rockbridgeite cell dimensions closely match those reported previously by Lindberg (1949), but we do not agree on the interpretation of the space group. My films and crystal structure analysis support the space group *Bbmm*.

Laubmannite was first named and described by Frondel (1949). Its type locality is Buckeye Mountain, near Shady, Polk Co., Arkansas. The mineral occurs as radial discoidal aggregates of fibers, rich yellowish-green in color. During the course of this study, a new locality was discovered, the laubmannite occurring as bright yellow-green aggregates and affording a powder pattern virtually identical with the Arkansas material. The location is Leveäniemi in the Svappavaara mining district, Norrbotten Province, Sweden and the specimens were collected by Prof. F. E. Wickman in 1957. The specimens are preserved in the collection of the Swedish Natural History Museum, and occur in vugs in a gossan zone surrounding magnetite ore.

Single crystals of Arkansas laubmannite were obtained from specimens I personally collected and from specimens of a cotype collected and kindly donated by Mr. A. Kidwell. The crystals are small (about 50 microns in greatest dimension) but yielded good rotation and Weissenberg photographs. The resulting data presented in Table 2 conflict with the conclusion of Mrose (1955) that laubmannite is isostructural with dufrenite. Frondel (1949) states that laubmannite is isostructural with andrewsite on the basis of similar molecular ratios and powder patterns, but Claringbull and Hey (1958) offer cell criteria for andrewsite which indicate isotypy with rockbridgeite! The status of andrewsite remains questionable and further study on type material will be required. I observed the appearance of a darker green zone, especially near the tips of the fibers on many laubmannite specimens from Arkansas. The darker green mineral is conclusively dufrenite on the basis

TABLE 2. CRYSTAL CELL DATA OF SOME BASIC IRON PHOSPHATES

	a	b	c	β	Space group	Z	Formula	Location
Dufrenite[a]	25.84 (2) Å	5.126 (3)	13.78 (1)	111.20 (6)°	$C2/c$	4	$Ca_{\sim 0.5}Fe_6(OH)_6(H_2O)_2(PO_4)_4$	Cornwall, England
Rockbridgeite	13.783 (12)	16.805 (9)	5.172 (4)	—	$Bbmm$	4	$Fe^{2+}Fe_4^{3+}(OH)_5(PO_4)_3$	Irish Creek, Va.
Laubmannite	13.95 (2)	30.77 (4)	5.16 (1)	—	$Pbma$	4	$Fe_9^{3+}(OH)_{10}(PO_4)_4$	Buckeye Mtn., Ark.
Mineral A	14.0	38.3	5.14		$Pbma$ (?)	?	?	Fodderstack Mtn., Ark.
Beraunite[b]	20.80 (3)	5.156 (5)	19.22 (6)	93.34 (35)°	$C2/c$	4	$Fe^{2+}Fe_5^{3+}(OH)_5(H_2O)_4(PO_4)_4 \cdot 2H_2O$	Palermo #1 Mine, N.H.
Lipscombite[c]	5.37	—	12.81	—	$I4_122$	2	$Fe^{2+}Fe_2^{3+}(OH)_2(PO_4)_2$	synthetic
Lipscombite[d]	7.35 (2)	—	12.71 (3)	—	$P4_12_12$	4	$Fe^{2+}Fe_2^{3+}(OH)_2(PO_4)_2$	Fodderstack Mtn., Ark.
Barbosalite[e]	7.25 (2)	7.46 (2)	7.49 (2)	120.25 (9)	$P2_1/c$	2	$Fe^{2+}Fe_2^{3+}(OH)_2(PO_4)_2$	Minas Gerais, Brazil
Souzalite	12.58	5.10	13.48	113.0°	$A2/m$ or $A2$	2	$(Al, Mg, Fe)_6Al(OH)_6(PO_4)_4 \cdot 2H_2O$	Minas Gerais, Brazil
Cacoxenite[f]	27.59	—	10.45	—	$P6_3/m$ or $P6_3$	6	$Fe_{24}(OH)_{15}(H_2O)_8(PO_4)_{17} \cdot 15H_2O$	Shady, Ark.

[a] Mrose (1955) reports a 24.6, b 5.14, c 13.87 Å, β 100.42°, $P2_1/n$. Note dufrenite in I-setting gives a 24.5, c 13.8 Å, β 100.5°.

[b] Deep green crystal. Fanfani and Zanazzi (1967) give a 20.646 (5), b 5.129 (7), c 19.213 (5), β 93.62 (8)° for reddish material. Note one-half obtuse diagonal for a and c=13.6 Å.

[c] Data of Katz and Lipscomb (1951).

[d] Lindberg (1962) reports a 7.40, c 12.81 Å for manganoan-lipscombite from Sapucaia Pegmatite, Brazil.

[e] Data of Lindberg and Christ (1959). Note a_I=12.9 and $c_I/2$=5.2 Å. See text for notation.

[f] Halving a and c yield 13.80 and 5.22 Å respectively.

of powder and single crystal studies, whereas the more yellow-green material is laubmannite. This suggests that Mrose probably investigated a durfrenite occurring in close association with the laubmannite.

Data for mineral A, certainly a new species, are also listed in Table 2. The specimen studied was collected by Mr. A. Kidwell from a prospect on Fodderstack Mountain, Montgomery Co., Arkansas. Considerable effort was expended attempting to obtain single crystal material, but the mineral occurs only in the finest fibers, yielding a 5.12 Å fiber length and nearly unintelligible Weissenberg photographs. Thus, the crystal cell data, though probably correct, are tentative.

Souzalite, though not a basic iron phosphate, was investigated because the chemical analysis and physical properties reported by Pecora and Fahey (1949) suggested a relationship with these minerals. Single crystals of the type specimen from the Corrego Frio Pegmatite, Minas Gerais, Brazil (U. S. National Museum No. C5863), kindly donated by Dr. George Switzer, were investigated by oscillation, rotation and Weissenberg techniques. These results in Table 2 show that souzalite is a Mg-Al phosphate related to dufrenite. The crystal chemistry of souzalite is discussed in more detail in the section on the dufrenite structure.

Powder Data. All existing powder patterns of dufrenite, rockbridgeite, laubmannite and beraunite quoted in the literature are unreliable. To overcome the difficulties encountered in materials with at least one perfect cleavage direction such as the aforementioned species, pure fibers separated near the location of the examined single crystals were ground in acetone, then rolled into a sphere mount using rubber cement. The 114.6 mm diameter films were standardized with internal silicon (a 5.4301 Å). On the basis of the three-dimensional single crystal data, the powder lines were unambiguously indexed. This method of matching powder intensity with single crystal intensity also demonstrated that preferred orientation was eliminated during the course of sphere mount preparation. On the other hand, powder patterns obtained from rolled cylinders or from glass slide smears showed severe preferred orientation effects, no doubt contributing to the conflicting data reported in the literature. The indexed powder data for these species were then used for a least-squares refinement of the cell parameters.

Indexed powder data for dufrenite, rockbridgeite, laubmannite and beraunite, and unindexed data for mineral A are given in Table 3. It is clear that the low-angle reflections offer a good means for distinguishing these species. The dufrenite pattern corresponds to the pattern cited by Frondel (1949), although differences exist in relative intensities, probably due to preferred orientation in his material. The rockbridgeite data are similar to those reported by Lindberg (1949). The laubmannite data do not agree at all with the previously reported pattern of Frondel (1949). Frondel's data are very similar to those for dufrenite, suggesting inadvertent powder examination of that mineral. One might propose that type laubmannite is not a valid species but merely a variety of dufrenite, while my material is deserving of a new name. However, Frondel's published chemical analysis and proposed molecular formula do not conform with any dufrenite formula or computation based on its cell criteria. On the other hand, his laubmannite analysis conforms well with the cell criteria obtained for Arkansas material. Since chemical analysis usually requires a substantial quantity of material, it is probably based on true laubmannite, whereas the powder study was performed on adjacent dufrenite.

The powder pattern for beraunite is similar to that previously reported by Frondel (1949), except for considerable differences in relative intensities. My beraunite is from the Palermo No. 1 Pegmatite and these data, with the exception of a slightly expanded cell, agree closely with those obtained from the more typical reddish-orange oxidized varieties

TABLE 3. X-RAY POWDER PATTERNS OF SOME BASIC IRON PHOSPHATES

DUFRENITE

I/Io	*d*(obs.)	*d*(calc.)	*hkl*	*I/Io*	*d*(obs.)	*d*(calc.)	*hkl*
9	12.00	12.045	200	1	1.8767	1.8744	$\bar{8}24$
2	6.783	6.778	$\bar{2}02$	1	1.8198	1.8196	$\bar{10}.2.2$
3	6.407	6.426	002	1	1.7645	1.7618	11.1.2
2	5.994	6.022	400	2	1.7503	1.7483	$\bar{9}17$
9	5.002	5.014	110			1.7440	$\bar{13}.1.5$
2	4.795	4.795	$\bar{1}11$	2	1.7232	1.7215	$\bar{6}08$
4	4.350	4.360	$\bar{3}11$			1.7207	14.0.0
5	4.110	4.106	$\bar{1}12$	1	1.7004	1.6948	$\bar{6}26$
2	3.763	3.767	402	1	1.6772	1.6769	715
3	3.630	3.639	$\bar{5}11$	2	1.6520	1.6476	$\bar{8}26$
1	3.508	3.511	510			1.6473	$\bar{12}.2.2$
7	3.393	3.389	$\bar{4}04$	1	1.6247	1.6239	$\bar{7}18$
		3.389	$\bar{3}13$			1.6224	$\bar{15}.1.2$
5	3.214	3.213	004			1.6222	$\bar{5}31$
		3.209	$\bar{8}02$	2	1.6105	1.6064	008
10	3.151	3.153	$\bar{5}13$			1.6044	$\bar{16}.0.4$
4	2.990	2.986	$\bar{7}11$	5	1.5749	1.5765	$\bar{10}.2.6$
6	2.860	2.858	$\bar{3}14$			1.5712	$\bar{5}33$
2	2.795	2.802	$\bar{1}14$			1.5711	226
		2.787	512	1	1.5534	1.5537	13.1.2
4	2.627	2.627	711	2	1.5226	1.5194	532
2	2.565	2.563	020	3	1.4972	1.4970	11.1.4
1	2.487	2.486	404			1.4927	$\bar{14}.2.2$
3	2.427	2.426	$\bar{3}15$	1	1.4691		
		2.426	221	1	1.4531		
		2.421	513	1	1.4462		
		2.412	802	1	1.4235		
3	2.409	2.409	10.0.0	1	1.4049		
1	2.362	2.367	314	1	1.3946		
1	2.277	2.278	222	1	1.3861		
1	2.223	2.220	115	1	1.3743		
1	2.150	2.151	$\bar{8}06$	1	1.3628		
		2.150	$\bar{12}.0.2$	1	1.3455		
5	2.101	2.099	$\bar{11}.1.1$	1	1.3321		
3	2.055	2.053	$\bar{2}24$	1	1.3165		
2	2.008	2.007	12.0.0	2	1.2952		
		2.003	$\bar{8}22$	1	1.2697		
2	1.9897	1.9885	206	1	1.2601		
3	1.9389	1.9370	622	1	1.2497		
1	1.9061	1.9080	224				

TABLE 3—(*Continued*)

ROCKBRIDGEITE

I/Io	*d*(obs.)	*d*(calc.)	*hkl*	*I/Io*	*d*(obs.)	*d*(calc.)	*hkl*
						1.7139	810
3	8.41	8.40	020	2	1.7081	1.7047	272
4	6.87	6.89	200	3	1.6805	1.6805	0.10.0
1	6.40	6.38	210	1	1.6133	1.6141	303
5	4.842	4.842	101	5	1.5890	1.5876	1.10.1
4	4.630	4.653	111	2	1.5514	1.5502	680
2	4.352	4.347	230	3	1.5298	1.5293	652
3	4.180	4.201	040	1	1.5097	1.5104	4.10.0
		4.195	121			1.5067	343
2	3.676	3.663	131	2	1.4778	1.4786	292
5	3.573	3.587	240	2	1.4578		
4	3.433	3.435	301	2	1.3927		
4	3.364	3.365	311	1	1.3697		
10	3.196	3.180	321	1	1.3418		
3	3.016	3.021	250	3	1.2945		
2	2.934	2.935	430	1	1.2544		
		2.928	331	1	1.2312		
4	2.754	2.761	151	1	1.2184		
2	2.663	2.664	440	1	1.2101		
3	2.584	2.586	002	1	1.1872		
5	2.409	2.402	351	1	1.1650		
1	2.332	2.337	521	2	1.1487		
2	2.262	2.267	270	2	1.0895		
1	2.214	2.216	620	1	1.0760		
		2.202	042	1	1.0670		
2	2.148	2.151	171	1	1.0362		
3	2.103	2.101	080	1	1.0287		
		2.098	242	1	1.0063		
4	2.052	2.053	412	1	0.9956		
2	2.015	2.016	640	1	0.9880		
3	1.9624	1.9645	252	1	0.9841		
4	1.8333	1.8317	262	1	0.9815		
2	1.7925	1.7936	480	1	0.9795		
1	1.7190	1.7174	602				

LAUBMANNITE

I/Io	*d*(obs.)	*d*(calc.)	*hkl*	*I/Io*	*d*(obs.)	*d*(calc.)	*hkl*
9	15.30	15.38	020	5	4.779	4.781	111
4	7.65	7.69	040	1	4.638	4.617	121
4	6.86	6.80	210	4	4.115	4.131	260
2	6.32	6.35	220			4.111	211
10	5.150	5.166	240	4	3.990	4.005	221
		5.161	001	7	3.716	3.718	270

TABLE 3—(*Continued*)

I/Io	*d*(obs.)	*d*(calc.)	*hkl*	*I/Io*	*d*(obs.)	*d*(calc.)	*hkl*
7	3.446	3.464	410			1.8537	2.16.0
		3.454	301	2½	1.8364	1.8387	2.15.0
6	3.273	3.301	430	1	1.7455	1.7432	800
		3.273	331	2	1.7062		
7	3.151	3.151	341	1	1.6647		
5	3.012	3.012	351	5	1.6120		
5	2.817	2.815	2.10.0	2	1.5930		
5	2.798	2.792	191	2	1.5751		
3	2.580	2.583	480	3	1.5473		
4	2.428	2.423	521	2	1.5141		
		2.421	1.11.1	1	1.4734		
3	2.303	2.305	062	1	1.4636		
1	2.261	2.267	630	1	1.4473		
3	2.143	2.142	571	2	1.4106		
1	2.108	2.114	611	1½	1.3619		
3	2.070	2.074	402	1½	1.3273		
		2.069	412	1	1.3007		
		2.068	581	2	1.2912		
3	2.027	2.033	432	1	1.2662		
3½	1.9703	1.9752	292	1	1.2376		
		1.9655	452	1	1.2206		
3½	1.9069	1.9090	671	2	1.1425		
2	1.8513	1.8546	6.10.0	1	1.0859		

BERAUNITE

I/Io	*d*(obs.)	*d*(calc.)	*hkl*	*I/Io*	*d*(obs.)	*d*(calc.)	*hkl*
10	10.37	10.38	200	2	2.488	2.486	$\bar{2}21$
5	9.58	9.59	002	2	2.422	2.419	515
5	7.229	7.260	$\bar{2}02$	2½	2.312	2.315	$\bar{7}14$
1	5.184	5.192	400	2	2.227	2.227	$\bar{4}08$
6	4.825	4.825	111	1	2.154	2.154	423
5	4.418	4.411	112	3	2.109	2.106	$\bar{3}18$
2	4.091	4.071	$\bar{3}11$	1	2.082	2.080	$\bar{9}12$
3	3.747	3.750	312			2.077	10.0.0
3	3.468	3.487	$\bar{1}14$	1	2.058	2.060	424
		3.461	600	3	2.009	2.007	622
2	3.417	3.418	313	1	1.9718	1.9696	$\bar{5}18$
1	3.326	3.318	$\bar{6}02$	3	1.9232	1.9231	$\bar{6}24$
4	3.187	3.187	$\bar{3}14$	1	1.8697		
6	3.082	3.079	314	1	1.8302		
2	2.838	2.835	513	1	1.8128		
3	2.732	2.732	604	1	1.7838		
3	2.705	2.711	$\bar{1}16$	1	1.7671		
3	2.582	2.578	020	1	1.7423		

TABLE 3—(*Continued*)

I/Io	*d*(obs.)	*d*(calc.)	*hkl*	*I/Io*	*d*(obs.)	*d*(calc.)	*hkl*
2	1.7175			2	1.4364		
1½	1.6912			1	1.3715		
1	1.6622			1	1.3276		
1	1.6405			1	1.3151		
3	1.6209			2	1.2901		
1	1.5985			2	1.2790		
1	1.5700			1	1.2400		
2	1.5408			1½	1.2114		
2	1.4594						

MINERAL A

I/Io	*d*(obs.)	*d*(calc.)	*hkl*	*I/Io*	*d*(obs.)	*d*(calc.)	*hkl*
9	9.49			2	1.9089		
2	6.89			2	1.8558		
4	6.38			1	1.8170		
1	5.44			2	1.7373		
5	5.13			1	1.7116		
3	4.79			1	1.6918		
3	4.54			1	1.6635		
2	4.09			2	1.6460		
4	4.02			2	1.6023		
3	3.826			3	1.5934		
3	3.644			1	1.5634		
8	3.425			2	1.5485		
10	3.189			1	1.5226		
4	2.086			1	1.5122		
2	2.959			2	1.4883		
3	2.851			1	1.4646		
2	2.788			1	1.4274		
3	2.578			2	1.3990		
2	2.487			1	1.3880		
2	2.418			3	1.3285		
2	2.400			3	1.2920		
1	2.287			2	1.2704		
1	2.187			1	1.2266		
2	2.067			1	1.2109		
2	2.050			2	1.1776		
1	2.003			1	1.0864		
1	1.9519						

TABLE 3—(*Continued*)

LIPSCOMBITE (L) AND MINERAL A (A)

	I/Io	*d*(obs.)	*d*(calc.)	*hkl*		*I/Io*	*d*(obs.)	*d*(calc.)	*hkl*
A	4	9.48			A	1½	1.7439		
A	2	6.41			L	1	1.7120	1.7141	117
?	2	6.17			L	5	1.6600	1.6709	332
L, A	2½	5.176	5.195	110	L	3	1.6036	1.6032	333
L	3	4.803	4.809	111	L	5	1.5932	1.5907	422
			4.807	102				1.5903	404
A	1	4.560			L	2	1.4485	1.4411	510
A	2	4.042			L	1	1.4306	1.4307	317
A	1	3.845						1.4303	218
A	2	3.441			L	1	1.3754	1.3799	425
L	10	3.305	3.283	113		1	1.3657	1.3645	520
L, A	6	3.188	3.181	202				1.3643	513
A	1	3.096			L	1	1.3071	1.3115	318
A	2	2.812			L	3	1.2976	1.2989	440
L	4	2.586	2.598	220				1.2988	523
A	1	2.507						1.2983	426
A	2	2.435						1.2975	219
L	2	2.396	2.405	301	L	2	1.2247	1.2247	600
			2.403	204	L	1½	1.2090	1.2079	533
L	4	2.278	2.285	302	L	2	1.1604	1.1608	329
			2.283	115	L	1½	1.1372	1.1416	2.2.10
L	5	2.039	2.037	313	L	2	1.0934	1.0945	339
L	2	2.017	2.011	224	L	1	1.0650	1.0605	633
A	1	1.9041			L	2	1.0231	1.0247	3.3.10
A	2	1.8576			L	2	1.0186	1.0187	626
L	2½	1.8328	1.8351	206	L	2	1.0095	1.0092	713

("eleonorite") from Arkansas and Pennsylvania. This is consistent with the color of the mineral, which is dark greenish-black, indicative of some iron in the ferrous state. Indeed, the lower indices of refraction determined by Mrose on the Palermo beraunite cited in Palache, Berman and Frondel (1951) conform to beraunite with some iron in the ferrous state. Refined cell data for Palermo beraunite based on these powder data appear in Table 2 along with those data for the reddish-orange variety studied by Fanfani and Zanazzi (1967).

The powder data for mineral A are similar to many of the lines recorded by Frondel (1949) for an unknown altered basic iron phosphate from Waldgirmes, Saxony and are believed to represent the same species. These data were not indexed because of the poor quality of the single crystal photographs. Mineral A is a common hydrothermally reworked product of rockbridgeite and constitutes the major portion of the friable yellowish-brown outer zone of the Virginia rockbridgeite material described by Frondel. This new species is presently being studied by Mrose (priv. comm.).

DUFRENITE: ITS CRYSTAL STRUCTURE

Experimental Procedure. A flat wedge-shaped crystal measuring approximately 0.30×0.30 ×0.08 mm and having 0.0070 mm³ polyhedral volume was selected for study. Nearly all other crystals, though seemingly single to the eye, proved to be severely warped, prohibiting the collection of suitable intensity data; although minor streaking was present, this crystal gave reasonably good spot shapes on films. 1620 independent reflections of the *h*0*l* to *h*4*l* levels to $2\theta=60°$ were gathered on a manual Weissenberg geometry diffractometer using Zr-filtered Mo radiation. Only 720 reflections were above the background error ("non-zero") and were used in the ensuing analysis. The intensity data were corrected for differential absorption using a polyhedral correction program of Knowles and Stephenson (priv. comm.).

Solution of the Structure. The three-dimensional Patterson map, $P(xyz)$, and the projection, $P(xz)$, were prepared for vector set analysis. On account of the short [010] fiber axis, this analysis was largely confined to $P(xz)$. Solution of the structure proved difficult: several sets of plausible solutions yielded R_{h0l} between 0.40 and 0.45 based only on Fe and P and assuming an empirical cell formula $Fe_{24}P_{16}O_{96}H_{20}$. Despite these encouraging convergences, the electron density maps did not reveal sensible oxygen locations and densities. I then discovered the paper by Fanfani and Zanazzi (1967) who presented the solution of the beraunite structure, a related basic iron phosphate with similar cell criteria. That structure possesses a face-sharing octahedral triplet, the axis of which lies in the plane of the projection. This cluster, along with the associated phosphate groups, allowed for reinterpretation and relabelling of the vectors, which were consistent with an assumed octahedral triplet similarly oriented in dufrenite. The correct model gave $R_{h0l}=0.38$ for metals only; difference synthesis revealed all oxygen atoms associated with the metals and yielded the essential topology of the structure. Computation of the *y*-coordinates led to the full three-dimensional data, and least-squares atomic parameter refinement converged to $R_{hkl}=0.20$ for observed reflections only. At this stage, four iron, two phosphorus, and twelve oxygen atoms constituted the asymmetric unit.

Three-dimensional Fourier synthesis showed additional electron density on the two-fold rotor at O *y* $\frac{1}{4}$, with $y\approx-0.20$, situated at the center of a large hole in the structure. At first, this was believed to be a water molecule which was not directly associated with any metals. However, the distances to the nearest neighbor oxygen atoms were within 2.5 Å, too short for a hydrogen-bonded system. Furthermore, all available reliable chemical analyses of dufrenite do not indicate water beyond the amount already attributed to ligands. These analyses do show the presence of 'impurities', such as CaO, Na_2O and MnO. Thus, this site was assumed to be a trap for larger more loosely-held cations. Addition of the electron density equivalent of two calcium atoms in the unit cell—half a calcium atom at the O *y* $\frac{1}{4}$ site—brought R_{hkl} down to 0.17. Three-dimensional refinement of atomic coordinates and isotropic temperature factors converged to 0.13 for the 720 observed reflections and 0.19 for all reflections. Final atomic parameters are given in Table 4 and the $|F_{obs}|$-F_{calc} data appear in Table 5.[1]

Crystallochemical Formula. Based on this crystal structure analysis, the

[1] To obtain a copy of Table 5, order NAPS Document #00747 from ASIS National Auxiliary Publications Service, c/o CCM Information Sciences, Inc., 22 West 34th Street, New York, New York 10001; remitting $1.00 for microfiche or $3.00 for photocopies payable to ASIS-NAPS.

TABLE 4. DUFRENITE AND ROCKBRIDGEITE: FORMULA UNIT MULTIPLICITIES, ATOMIC COORDINATES, AND ISOTROPIC TEMPERATURE FACTORS. (ESTIMATED STANDARD ERRORS IN PARENTHESES)

	M	*x*	*y*	*z*	B(Å²)
DUFRENITE					
Fe (1)	1	0	0	0	1.15 (8)
Fe (2)	1	¼	¼	0	1.25 (8)
Fe (3)	2	0.1529 (1)	−0.0150 (8)	0.1116 (3)	1.01 (6)
Fe (4)	2	.1401 (2)	− .2220 (8)	.3545 (3)	1.18 (6)
P (1)	2	.2185 (3)	.2612 (13)	.3312 (5)	1.20 (9)
P (2)	2	.0790 (3)	.2808 (14)	.3970 (5)	1.38 (10)
Ca	0.5	0	− .1474 (28)	¼	1.78 (20)
O (1)	2	.0887 (7)	.0660 (34)	.3293 (13)	1.14 (26)
O (2)	2	.0769 (8)	.5468 (39)	.3422 (15)	1.77 (31)
O (3)	2	.0193 (8)	.2255 (38)	.4030 (14)	1.85 (30)
O (4)	2	.1224 (8)	.2896 (37)	.5055 (14)	1.60 (29)
O (5) = OH^-	2	.1727 (8)	.2183 (37)	.0170 (14)	1.58 (29)
O (6)	2	.2134 (8)	.0108 (36)	.3878 (14)	1.47 (28)
O (7)	2	.2029 (8)	− .5144 (38)	.3907 (15)	2.13 (31)
O (8) = OH^-	2	.1289 (9)	− .2574 (39)	.2046 (15)	1.85 (33)
O (9)	2	.1766 (8)	.2529 (36)	.2203 (14)	1.75 (29)
O (10)	2	.2223 (8)	− .2034 (36)	.1670 (14)	1.62 (28)
O (11) = OH^-	2	.0769 (8)	.1439 (38)	.0645 (14)	2.07 (30)
O (12) = H_2O	2	.0243 (9)	− .2853 (41)	.1119 (16)	2.25 (34)
ROCKBRIDGEITE					
Fe (1)	1	0	0	0	0.10 (9)
Fe (2)	2	0.0687 (5)	0.1574 (4)	0	1.64 (9)
Fe (3)	2	.3214 (4)	.1385 (3)	0.2385 (14)	0.10 (8)
P (1)	2	.1420 (6)	.0432 (5)	½	0.08 (11)
P (2)	1	.4806 (10)	¼	0	0.76 (19)
O (1)	2	0.0477 (19)	¼	0.2508 (66)	2.38 (43)
O (2)	4	.0829 (10)	0.0605 (8)	.2615 (32)	0.56 (20)
O (3) = OH	1	.3132 (31)	¼	.3876 (95)	0.81 (57)
O (4)	2	.3126 (22)	.0357 (18)	0	1.86 (51)
O (5) = OH	2	.2175 (18)	.1720 (14)	0	0.75 (37)
O (6) = OH	2	.4204 (18)	.1071 (14)	½	0.31 (37)
O (7)	2	.4171 (18)	.1763 (15)	0	0.91 (37)
O (8)	2	.2276 (16)	.1044 (13)	½	(0.10) (33)[a]

[a] Refined to B = −0.04.

unit cell of dufrenite contains $X_2Fe_{24}P_{16}O_{96}H_{40}$, where X is essentially Ca^{2+}, according to the analysis of Kinch in Kinch and Butler (1886) for Cornish dufrenite crystals. The crystallochemical computation based

TABLE 6. DUFRENITE AND ROCKBRIDGEITE: CHEMICAL ANALYSES

	DUFRENITE		
	1	2	3
CaO	1.50	3.21	—
FeO		8.23	—
Fe_2O_3	55.63	45.73	56.16
P_2O_5	30.26	32.51	33.28
H_2O	10.62	10.32	10.56
Rem.	1.48	—	—
	99.49	100.00	100.00

1. Analysis of Kinch in Kinch and Butler (1886). Rem. is SiO_2 0.53 and CuO 0.95.
2. $CaFe_2^{2+}Fe_{10}^{3+}(OH)_{12}(H_2O)_4(PO_4)_8$
3. $Fe_6^{3+}(OH)_6(H_2O)_2(PO_4)_4$

	ROCKBRIDGEITE		
CaO	1.12	—	
FeO	6.14	11.07	—
Fe_2O_3	50.84	49.20	61.60
P_2O_5	31.76	32.80	32.85
H_2O	8.53	6.93	5.55
Rem.	1.48	—	—
	99.87	100.00	100.00

1. Analysis of Campbell (881). Rem. is 0.76 MgO, 0.40 MnO, 0.21 Al_2O_3, 0.11 insoluble.
2. $Fe^{2+}Fe_4^{3+}(OH)_5(PO_4)_2$
3. $Fe_5^{3+}(O)(OH)_4(PO_4)_3$

on this analysis in Table 6 shows the good resolution between the crystal structure analysis and wet chemical analysis. Based on the evidence offered here, as well as discussion of valence states later on, the molecular formula for dufrenite ranges from

$$X^{1+}Fe^{2+}Fe^{3+}_5(OH)_6(H_2O)_2(PO_4)_4 \quad \text{to} \quad Fe^{3+}_6(OH)_6(H_2O)_2(PO_4)_4.$$

Topology and Topochemistry. The octahedral framework in the dufrenite structure is shown in Figure 1a. A face-sharing cluster of three octahedra is the underlying unit not only in the dufrenite structure, but also in the other basic iron phosphate structures. These clusters are joined along [100] by corner-sharing octahedral triplets and along [001] by individual members of this corner-sharing triplet. The phosphate tetrahedra, all of which are associated around the face-sharing three-cluster, further knit

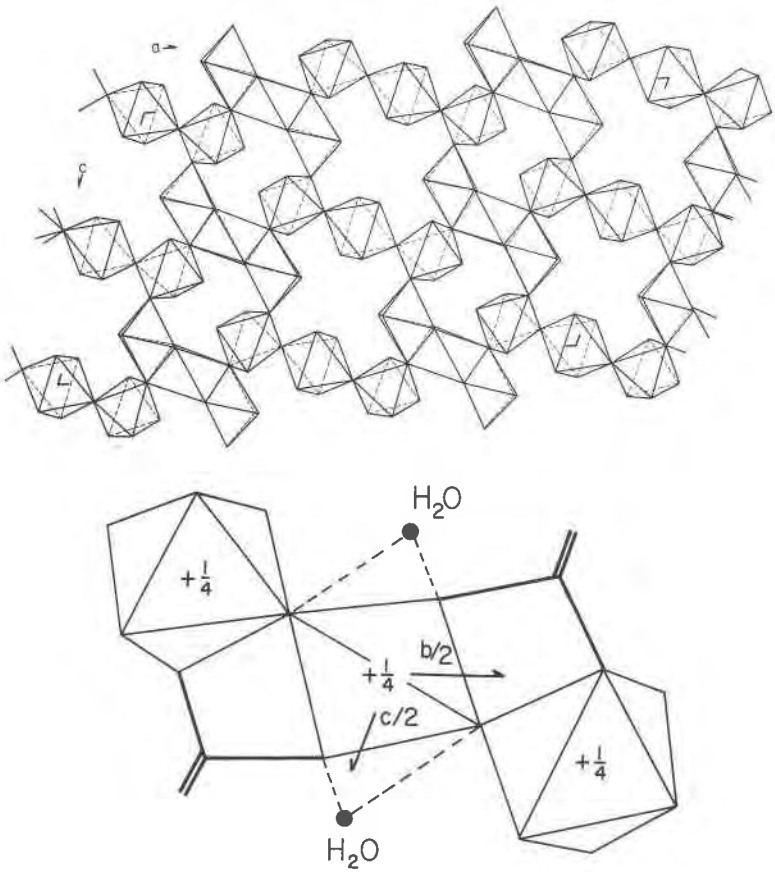

FIG. 1. Octahedral frameworks of dufrenite and souzalite. (a) The dufrenite octahedral structure down the *b*-axis. (b) Proposed model for the octahedral bridge in souzalite.

together this cluster and the corner-sharing triplets by corner-sharing. The $(PO_4)^{3-}$ tetrahedra secure the face-sharing triplets along [010], the fiber axis. The 5.13 Å axis, common to many basic ferrous-ferric phosphates, is approximately the sum of the phosphate tetrahedral edge and the octahedral edge belonging to the face-sharing cluster. Taken together, these clusters, the tetrahedra, and portions of the corner-sharing triplets make up a reasonably dense slab which is oriented parallel to {100}; this explains the perfect {100} cleavage observed for dufrenite.

This remarkable face-sharing three-cluster involves eight oxygen atoms from the $(PO_4)^{3-}$ tetradentate ligands and four hydroxyl groups. According to Moore (1965a), its formula can be written $Fe_3(OH)_4(O_p)_8$.

Further citing that paper, I shall refer to this cluster as the *h*-cluster, following the proposed code for octahedral clusters involving four or less nuclei. In the same fashion, the corner-sharing triplet, having composition $Fe_3(OH)_6(H_2O)_2(O_p)_8$, will be called the *e*-cluster. Thus, the octahedral framework in dufrenite involves the condensation and subsequent corner-sharing of *h*-clusters and *e*-clusters.

Remaining in the dufrenite structure is a fairly open cavity along the two-fold rotor at 0 *y* 1/4. This cavity is partly occupied in the Cornish dufrenite studied herein. It is believed to be occupied by calcium, since the analysis of Kinch indicates the presence of 1.5 percent CaO. A crude estimate of the average electron density can be obtained by the refinement of the isotropic temperature factor. Applying the scattering curve for half-occupied Ca^{2+} at this site, the isotropic temperature factor refined to 1.78 Å^2, a not unreasonable value for a large cation in a cavity. The interatomic X—O distances are 2 X—O(1) 2.41, 2 X—O(2) 2.49, 2 X—O(12) 2.32, and a long 2 X—O(3) 2.76 Å. The first six distances are reasonable values for Ca-O; discounting the long pair of distances, Ca^{2+} is in approximate octahedral coordination. The formula for Cornish dufrenite is then approximately $CaFe_{12}(OH)_{12}(H_2O)_4(PO_4)_8$, yielding a computed CaO of 3.1 percent by weight.

Though present evidence is inconclusive, I would like to suggest that dufrenite follows an oxidation trend analogous to the well-known triphylite-ferrisicklerite-heterosite series. Triphylite is commonly observed to follow a step-wise progressive oxidation, with retention of the essential crystal structure, from $LiFe^{2+}(PO_4)$ to $Fe^{3+}(PO_4)$, the ferric end-member being heterosite. The general formula expressing this series can be written $Li_xFe^{2+}{}_xFe^{3+}{}_{1-x}(PO_4)$, where progressive oxidation also involves concomitant alkali-leaching. In such a process, the electrostatic valence balance about the oxide anions is preserved. Quite analogous is dufrenite, since the electrostatic valence balance computation in Table 7 shows that only one water molecule is present in the asymmetric unit, this being O(12), with Σ, the electrostatic valence sum, $=0.50$ for the ferric end-member. The hydroxyl oxygens, OH(5), OH(8) and OH(11)all have $\Sigma=1.00$, a value too high for neutral water molecules. Thus, to achieve stability during oxidation of the dufrenite crystal, a commensurate amount of large cation is leached out of the structure. It now remains to obtain the limiting composition for the ferrous end-member in the dufrenite series, as discussed in the following section.

Interatomic Distances. The average Fe-O interatomic distances are Fe(1)—O 2.00, Fe(2)—O 2.06, Fe(3)—O 1.98, and Fe(4)—O 2.04 Å with estimated standard errors of ± 0.02Å. Those for Fe(1) and Fe(3)

TABLE 7. ELECTROSTATIC VALENCE BALANCES (Σ) OF DUFRENITE AND ROCKBRIDGEITE

Dufrenite				Rockbridgeite			
		Σ^a	Σ^b			Σ^a	Σ^b
O (1)	P(2)+Fe(4)	1.70	1.75	O (1)	P(2)+Fe(2)+Fe(2)′	2.14	2.25
O (2)	P(2)+Fe(4)	1.70	1.75	O (2)	P(1)+Fe(1)+Fe(2)	2.14	2.25
O (3)	P(2)+Fe(1)	1.75	1.75	O (3) =OH⁻	Fe(3)+Fe(3)′	1.00	1.00
O (4)	P(2)+Fe(3)	1.75	1.75	O (4)	P(1)+Fe(3)	1.75	1.75
O (5) =OH⁻	Fe(2)+Fe(3)+Fe(4)	1.33	1.50	O (5) =OH⁻	Fe(1)+Fe(3)	1.00	1.00
O (6)	P(1)+Fe(2)+Fe(4)	2.14	2.25	O (6) =OH⁻	Fe(1)+Fe(2)+Fe(3)	1.33	1.50
O (7)	P(1)+Fe(2)+Fe(4)	2.14	2.25	O (7)	P(2)+Fe(3)	1.75	1.75
O (8) =OH⁻	Fe(3)+Fe(4)	0.94	1.00	O (8)	P(1)+Fe(3)	1.75	1.75
O (9)	P(1)+Fe(3)	1.75	1.75				
O (10)	P(1)+Fe(3)	1.75	1.75				
O (11) =OH⁻	Fe(1)+Fe(3)	1.00	1.00				
O (12) =H_2O	Fe(1)	0.50	0.50				

[a] For *h*-cluster iron atoms averaging +2.67 (based on 2 Fe^{3+}+Fe^{2+}).
[b] For ferric end members.

are normal distances for Fe^{3+}—O; similar values (1.98 and 1.98Å) were found for the two independent Fe^{3+}—(O, OH) octahedral averages in laueite (Moore, 1965b). The Fe(2) and Fe(4) octahedral distances associated with the *h*-cluster are indicative of the presence of some iron in the ferrous state. The electrostatic valence balance calculation in Table 7 shows that the three oversaturated oxide and hydroxyl anions—OH(5) =OH; O(6), O(7) = O_p—are associated with both Fe(2) and Fe(4). By lowering the average positive charge for these cations, the degree of over-saturation can be diminished. This, in combination with chemical analyses, suggests that the limit for the ferrous end-member is Fe^{2+}: Fe^{2+} +Fe^{3+} = 1:6. It is evident that the dufrenite used in this study represents partly oxidized material, but the limitations of the structure analysis do not warrant any accurate assessment of the degree of oxidation on the basis of interatomic distances. It appears likely that the Kinch analysis for Cornish dufrenite is incomplete and that some Fe^{2+} was present. Further support of this conclusion is gained by the dark green color of the crystals, a phenomenon indicative of electron transfer, thus involving mixed valence states of iron in the crystal. Color and oxidation grade will be discussed later under the general crystal chemistry of these compounds.

Finally, there are the P-O distances, which average 1.53 P(1)—O and 1.55 Å P(2)—OH, typical values for the $(PO_4)^{3-}$ tetrahedron. All M—O, T—O and O—O′ polyhedral distances are presented in Figures 4 and 5a, using Schlegel diagrams to represent these polyhedra. The Schlegel diagram of a polyhedron has the advantage of pictorially representing a three-dimensional object in two dimensions. It is drawn by generalizing the polygonal unit for the polyhedron and its topological graph is made

to conform with its associated polyhedron. In general, a Schlegel diagram can be found for any polyhedron of genus zero (Coxeter, 1947), that is, the family of closed convex polyhedra with no holes. These diagrams offer the advantage over tables in that M—O, O—O′ distances and angles can be conveniently inserted, easing the difficulty of relating tabular data to figures. The O—O′ distances are particularly interesting and offer us further insight into the *h*-cluster, as discussed later.

Souzalite: a probable dufrenite-like structure. Souzalite is a hydrothermally reworked product of scorzalite and occurs as bluish-green aggregates of polysynthetically twinned prismatic crystals. Its crystal chemistry reflects the parent scorzalite, but it differs in containing less alumina, less phosphate anion, more magnesia and more water. A crystal cell computation using Fahey's analysis in Pecora and Fahey (1949) based on 8P yields $Fe^{2+}_{2.4}Mg_{3.6}Fe^{3+}_{0.5}{}^{1}Al^{3+}_{7.7}P_{8.0}H_{20.2}O_{48.4}$. The crystal cell data in Table 2 indicate a close relationship between souzalite and dufrenite. The souzalite space group is either $A2/m$ or $A2$ whereas dufrenite is $C2/c$: b, c and β are similar for the two minerals, but a is halved in souzalite relative to dufrenite. Further evidence for a relationship is the observed similarity in intensities of the $h0$ levels for the two minerals.

I propose a plausible atomic arrangement for souzalite. This proposed structure has the same *h*-cluster orientation as in dufrenite, except that the cluster is centered at the cell origin. The *h*-clusters are linked in the same fashion along [001] resulting in dense slabs parallel to {100}, identical to those found in dufrenite and explaining the perfect {100} cleavage also observed for souzalite. The difference appears in the linking unit along [100]. Instead of the *e*-cluster, this unit consists of two terminal octahedra corner-linked to a central tetrahedron, as depicted in Fig. 1b. This is the only sensible polyhedron which can link the slabs along [100] for a dufrenite-related cell in space group $A2$ or $A2/m$.

Balancing charges, the souzalite formula is $(Mg_{3.6}Fe_{2.4})^{2+}(Al_{7.7}Fe_{0.5})^{3+}(OH)_{12.6}(PO_4)_{8.0}\cdot 3.8\ H_2O$. Since it is unlikely that the central tetrahedron shares edges, the space group is probably $A2$. The non-ligand water molecules reside in the cavity similar to the one encountered in dufrenite but which in souzalite dimensionally permits water molecules. With M for octahedral sites and T for tetrahedral sites (excepting phosphorus), the structure type formula for souzalite is $M^{VI}_6T^{IV}(OH)_6(PO_4)_4\cdot 2H_2O$, with M and T including Al, Mg, and Fe. More detailed crystal structure analysis will be required before a sensible ordering scheme can be proposed. The tentative positions of the water molecules in Figure 1b were located on the basis of geometrical limitations combined with hydrogen bond distances.

Rockbridgeite: Its Crystal Structure

Experimental procedure. A nearly equant greenish-black crystal of 80 microns mean dimension was selected from Irish Creek, Virginia material. Its small size necessitated long exposure (96 hours) Weissenberg photographs using Zr-filtered Mo radiation. Packets of three films were separated by aluminum foils and the intensity data were estimated by eye using a spot scale of fifteen intervals based on the strong (642) reflection. 491 independent reflections were obtained for the *hk*0 to *hk*5 levels, of which 340 were non-zero. These data were not corrected for differential absorption, since the crystal was of favorable size and shape.

Solution of the structure. Knowledge of the dufrenite structure led to rapid solution of the rockbridgeite atomic arrangement. The *h*-cluster and its associated $(PO_4)^{3-}$ tetrahedra were assumed present in the rockbridgeite structure and oriented by placing the cluster's symmetry center at the cell origin. The space group criteria were then applied and the solution was immediately obvious. The derived atomic coordinates for the metals were then referred to $P(xyz)$; all prominent vectors could be labelled and gave sufficiently accurate trial coordinates for refinement. The oxygen atoms were approximately located from a polyhedral model and their coordinates were adjusted on the basis of an ensuing three-dimensional Fourier synthesis.

Two space groups, *Bbmm* and *Bbm*2, conform to the systematic extinction criteria observed on films. Only *Bbm*2 can satisfactorily accommodate the cell contents, assuming a crystal with ordered and fully occupied sites. Only two atoms—Fe(3) and O(3)—militate against the centrosymmetric space group, assuming complete site occupancy. Refinement based on *Bbm*2 involved 15 independent atomic species, and converged to $R_{hkl}=0.14$ for observed reflections, but resulted in disappointingly high e.s.d's for Fe—O distances (± 0.06 Å). Computation of Fe—O and P—O interatomic distances showed that serious departures from expected values occurred, e.g. with P-O ranging from 1.43 to 1.70 Å.

It was then decided to refine the structure based on *Bbmm*, assuming that Fe(3) at x, y,$\sim 1/4$ only half-occupied its site. Full occupancy of this site would result in 28 iron atoms in the unit cell, instead of 20 as supported by chemical analysis (Table 6). Besides, fully occupied face-sharing columns of octahedra would run parallel to the *c*-axis. Several other arguments, including the Patterson synthesis, supported half-occupied Fe(3) sites and a centrosymmetric arrangement. Topologically and topochemically, there is no difference between occupancy at $x\ y\ 1/4$ and $x\ y\ 3/4$ since the neighboring oxygen atoms and the other cations reside on the mirror planes at $z=0$ and $1/2$. Thus, there should be no energetic differences between the two sites. Incomplete occupancy of equivalent Fe sites is well-documented by Katz and Lipscomb (1951) in the crystal structure of lipscombite, $Fe^{2+}Fe^{3+}{}_2(OH)_2(PO_4)_2$, where full occupancy would result in infinite face-sharing octahedral columns. In lipscombite, these sites are 75 percent occupied on the average, and the fractional occupancy is probably even lower for the more oxidized synthetic varieties.

In the space group *Bbmm*, only 13 independent atomic species are present: two sets of oxygen pairs become equivalent by reflection. These pairs were averaged, starting with the coordinates obtained from the noncentrosymmetric refinement. O(3) was assumed half-occupied at x, $1/4$, z (with $z\sim 0.38$); full occupancy requires that O(3) be situated at $z=1/2$, but this results in an unreasonably long Fe(3)-O(3) distance of 2.35 Å. Indeed, noncentric refinement at $z=1/2$ led to $B=5.6$ Å^2, the model with the half-occupied site at the general *z*-position further supported by a convergence to $B=0.8$ Å^2. Thus, O(3) is disordered in the same manner as Fe(3).

Full-matrix three-dimensional atomic coordinate and isotropic temperature factor refinement converged to $R_{hkl}=0.12$ for the observed reflections and 0.16 for all reflections. The final parameters are listed in Table 4 and the $|F_{obs}|$-F_{calc} data appear in Table 5 (see

footnote under dufrenite). The temperature factors are generally lower than those obtained for dufrenite and for the beraunite studied by Fanfani and Zanazzi (1967), and this effect may arise from the more close-packed nature of the rockbridgeite structure. These temperature factors for the rockbridgeite structure show anomalous differences (compare P(1) with P(2); Fe(1), Fe(3) with Fe(2); and O(8), which is negative), and several attempts were made to obtain more meaningful values by alternating coordinate refinements with scale factor refinements, etc. Similar anomalies were observed for the refinements in the noncentrosymmetric space group and it is believed that a strong correlation exists between the temperature factors and atomic coordinates for some atomic positions. For this reason, these temperature factors probably have little physical meaning.

Crystallochemical formula. The crystal structure analysis confirms the generally accepted rockbridgeite formula of Lindberg (1949). The crystallochemical computation in Table 6 based on the analysis of Campbell (1881) shows good agreement, except for a higher water content in the analyzed material. Analyzed rockbridgeites consistently show a slightly higher water content, probably reflecting the fibrous habit of the material, which may permit the presence of some occluded water. Based on available chemical analysis, it is proposed that a continuous series exists between unoxidized rockbridgeite and fully oxidized material:

$$Fe^{2+}Fe^{3+}{}_4(OH)_5(PO_4)_3 \quad \text{to} \quad Fe^{3+}{}_5(O)(OH)_4(PO_4)_3.$$

The electrostatic valence balance calculations in Table 7 show that O(6) is severely oversaturated with respect to an hydroxyl group but undersaturated with respect to O^{2-} for the oxidized end-member. OH(6) is probably an average of O^{2-} and OH^- anions, the ferric end-member more precisely written $Fe^{3+}{}_5(O_{1/2}, OH_{1/2})_2(OH)_3(PO_4)_3$.

Topology and topochemistry. The octahedral framework in the rockbridgeite structure is shown in Figure 2a. The centrosymmetric *h*-cluster is situated at the cell origin and joins to adjacent *h*-clusters by shared terminal edges, forming octahedral chains parallel to the *b*-axis. The fusion of the *h*-cluster by shared edges results in a more efficiently packed structure than those found in dufrenite and beraunite. The phosphate tetrahedra are situated around the *h*-cluster in a manner identical to that in dufrenite and beraunite. The cross-linking corner-sharing octahedra are doublets, analogous to the *b*-cluster of Moore (1965). These *b*-clusters have composition $Fe_2(OH)_5(O_p)_6$. Thus, the dense slabs found in the dufrenite and beraunite structures are preserved oriented parallel to $\{010\}$ in the rockbridgeite structure. However, the addition of edge-sharing elements along the *b*-axis results in the preferred cleavage direction parallel to $\{100\}$, *not* parallel to the slabs but perpendicular to them.

Rockbridgeite can be derived from the dufrenite and beraunite struc-

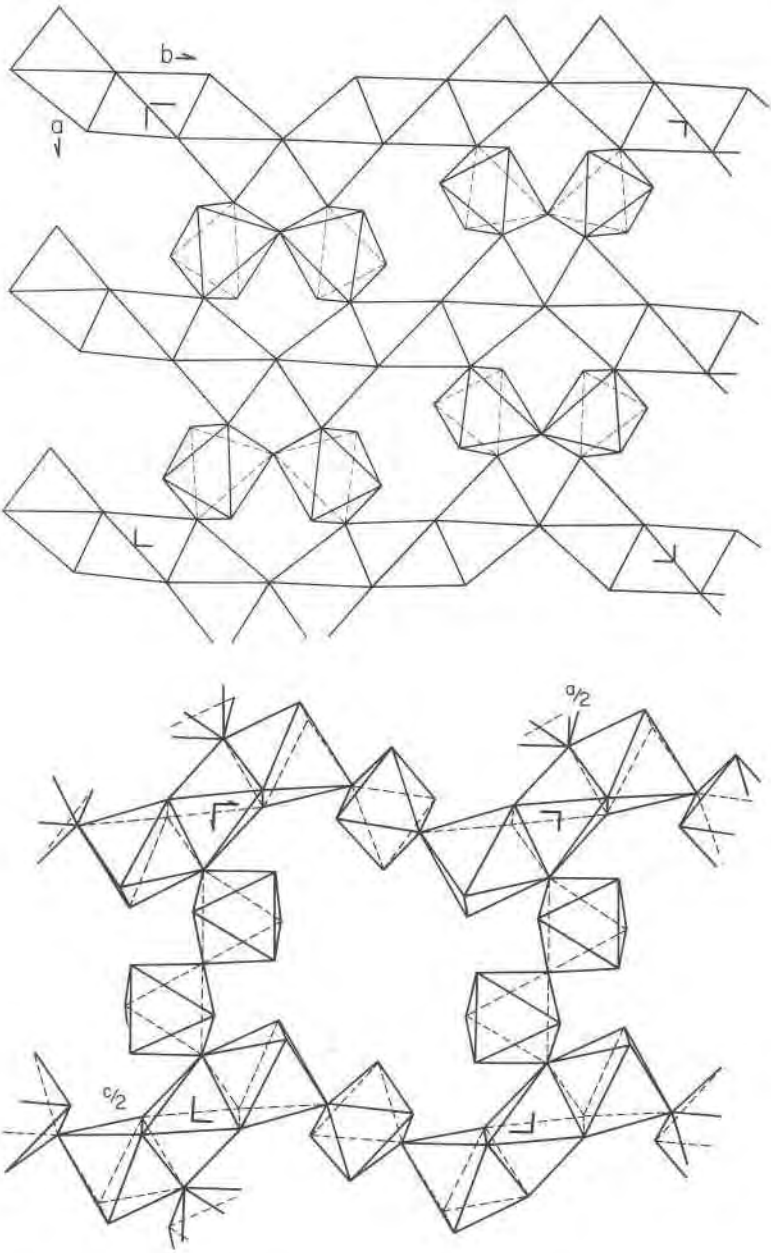

FIG. 2. Octahedral frameworks of rockbridgeite and beraunite. (a) The rockbridgeite octahedral structure down the *c*-axis. (b) Beraunite structure. Coordinates are from Fanfani and Zanazzi (1967).

tures by twinning through reflection parallel to the slabs. In this manner, one octahedron in the dufrenite *e*-cluster is removed, resulting in a *b*-cluster and in beraunite one octahedron is joined by corner-sharing to the *a*-cluster making it a *b*-cluster. As a consequence, the denser rockbridgeite appears to be a highly strained structure, possibly explaining the displacement of OH(3) away from the mirror plane at $z=1/2$.

Interatomic distances. The average Fe—O interatomic distances are Fe(1)—O2.07. F(2)—O2.11 and Fe(3)—O2.00 Å with estimated standard errors in individual distances ± 0.03 Å. Thus, Fe(3) is probably essentially ferric iron. Fe(1) and Fe(2) belong to the *h*-cluster and these distances are suggestive of mixed Fe^{2+} and Fe^{3+} over these sites. As with dufrenite, the oversaturated oxide and hydroxyl anions—O(1), O(2) and O(6)—are associated with both Fe(1) and Fe(2) in the *h*-cluster.

The P—O distances average P(1)—O1.52 and P(2)—O1.56 Å. The distances associated with O(4) are rather unusual: P(1)—O(4) 1.47 is unusually short, Fe(3)—O(4) 2.12 long, and O(4)—O(6) (with Fe(3)) 3.22 Å long; but the remaining polyhedral distances for O(4) are quite normal. Since O(4) is associated with the *b*-cluster bridged by phosphate tetrahedra, these distances may indicate a "forced" arrangement in the crystal structure. All M—O, T—O and O—O′ polyhedral distances are presented in Figures 4 and 5b as the Schlegel diagrams for the polyhedra.

Comparison of the dufrenite, rockbridgeite and beraunite polyhedral distances. The composite Schlegel diagrams (Figs. 4, 5a and 5b) for the polyhedra in the three related structures afford clear and concise means of illustrating distances for comparative purposes. The octahedra in the *h*-clusters for the three species are drawn so that a one-to-one correspondence exists in position. O—O′ distances for shared edges are consistently shorter than for the free edges. The central octahedron of the *h*-cluster for all three structures shows remarkable similarity in corresponding distances among these structures. This is because the central octahedron has the same nearest neighbors in the structures. The outer octahedra in the dufrenite and beraunite *h*-clusters are similar for the same reason, but in rockbridgeite differ because of the extra shared edge. In rockbridgeite, compensation of O—O′ distances is especially pronounced (compare the long $O(1)^{I}$—$O(6)^{III}$ and $O(1)^{I}$—$O(2)^{IV}$ with analogous edges in the other two species). The distances are substantially longer in the rockbridgeite *h*-cluster than in the other two sepcies, indicating more ferrous iron in that mineral. The remaining polyhedra in the three species cannot be compared because their nearest neighbor polyhedra are arranged differently.

The *h*-Cluster

The *h*-cluster is known to exist in the crystal structures of dufrenite, rockbridgeite, beraunite, lipscombite, barbosalite, laubmannite, and possibly mineral A. Beraunite, with the most open octahedral framework of these species, is closely related to dufrenite. The beraunite structural parameters possess fairly low estimated standard errors (Me—O $\pm$0.01 Å) as a result of careful study by Fanfani and Zanazzi (1967). The octahedral topology is shown in Figure 2b, and the cell criteria are offered in Table 2. Here, the *h*-cluster is corner-linked by octahedral *a*- and *b*-clusters. In a manner similar to dufrenite, the octahedra and tetrahedra form reasonably dense slabs oriented parallel to $\{100\}$, explaining the perfect $\{100\}$ cleavage plane observed for the mineral. The octahedral framework results in large open channels oriented parallel to the fiber axis and non-ligand water molecules occupy these channels; the crystallochemical formula for beraunite involves the series $Fe^{2+}Fe^{3+}_5(OH)_5(H_2O)_4(PO_4)_4\cdot 2H_2O$ to $Fe^{3+}_6(OH)_6(H_2O)_3(PO_4)_4\cdot 2H_2O$ and the electrostatic valence balance computations parallel those observed for dufrenite.

Lipscombite, $Fe^{2+}Fe^{3+}_2(OH)_2(PO_4)_2$, has an intriguing structure which was revealed by Katz and Lipscomb (1951), the polyhedral diagram of which appears in Figure 3a and the cell criteria in Table 2. Here, equivalent chains of face-sharing octahedra run parallel to the *a*-axes of the tetragonal cell. The octahedra are only partly occupied, with an average of 3/4 Fe per octahedron for the ratio $Fe^{2+}:Fe^{3+}=1:2$. These chains are actually face-fused *h*-clusters with a phosphate environment identical to that of the other basic iron phosphates. Lipscombite probably represents the densest arrangement of *h*-clusters among the basic iron phosphates, and can be considered a limiting structure for these compounds.

Gheith (1953) investigated the stability of the lipscombite structure through synthesis, using various starting materials. He showed that the lipscombite structure could be synthesized as the pure ferric end-member, with 5 1/3 Fe^{3+} per cell instead of 2 Fe^{2+}+4 Fe^{3+} for the 1:2 compound, but the analogous ferrous end-member (requiring completely occupied octahedral sites) could not be prepared.

It is tempting to add that an ordered derivative of the lipscombite structure could possibly exist, where one set of face-sharing chains is wholly intact and fully occupied by cations. To satisfy the lipscombite 1:2 stoichiometry, the other chain would reduce to the insular *a*-clusters which join to the phosphate tetrahedra and bridge the chains by corner-sharing. Because of the short Fe–Fe distances (about 2.7 Å) along the chain, such an arrangement may have unusual electrical properties. Presumably, the *a*-cluster would be occupied by a cationic species of different crystal radius, thus increasing the possibility of such an order-

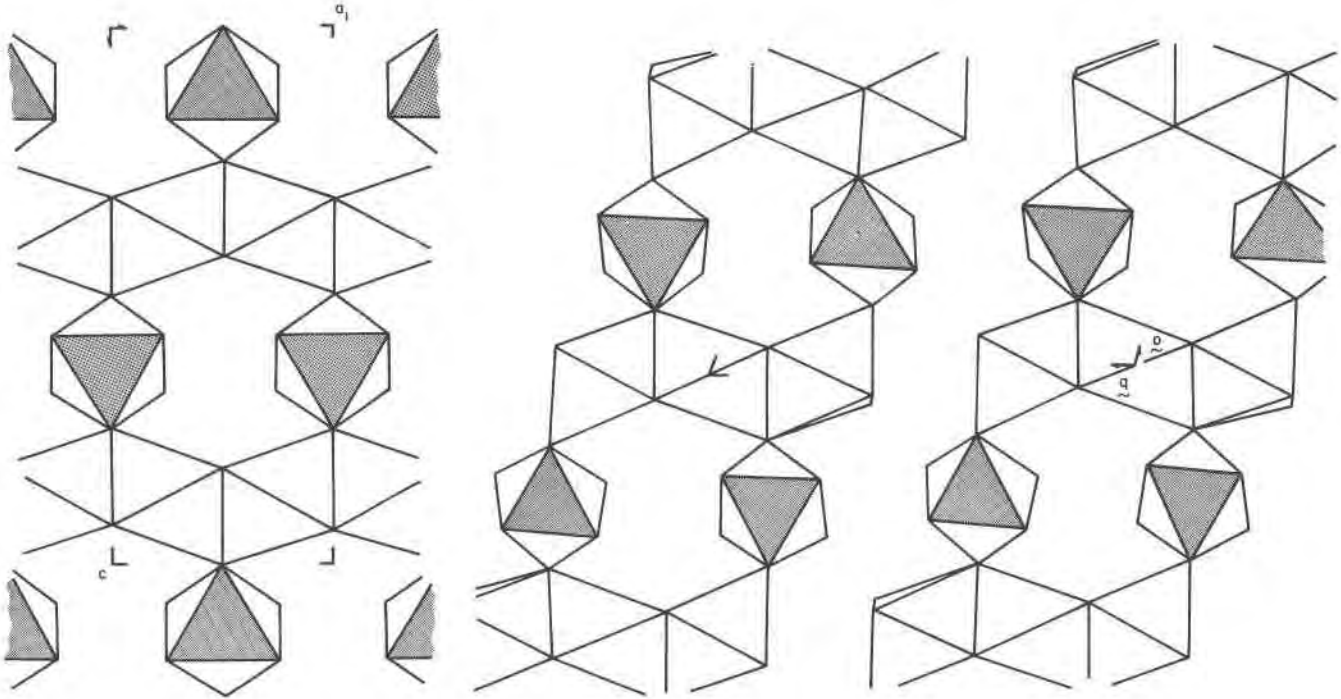

FIG. 3. Octahedral frameworks of lipscombite and barbosalite. (a) Lipscombite. The shared faces are stippled. Note the face-sharing chain parallel to a_1. The coordinates are from Katz and Lipscomb (1951). (b) Barbosalite. Shared faces in the octahedral triplet are stippled. See text for axial convention. Coordinates pertain to lazulite, in Lindberg and Christ (1959).

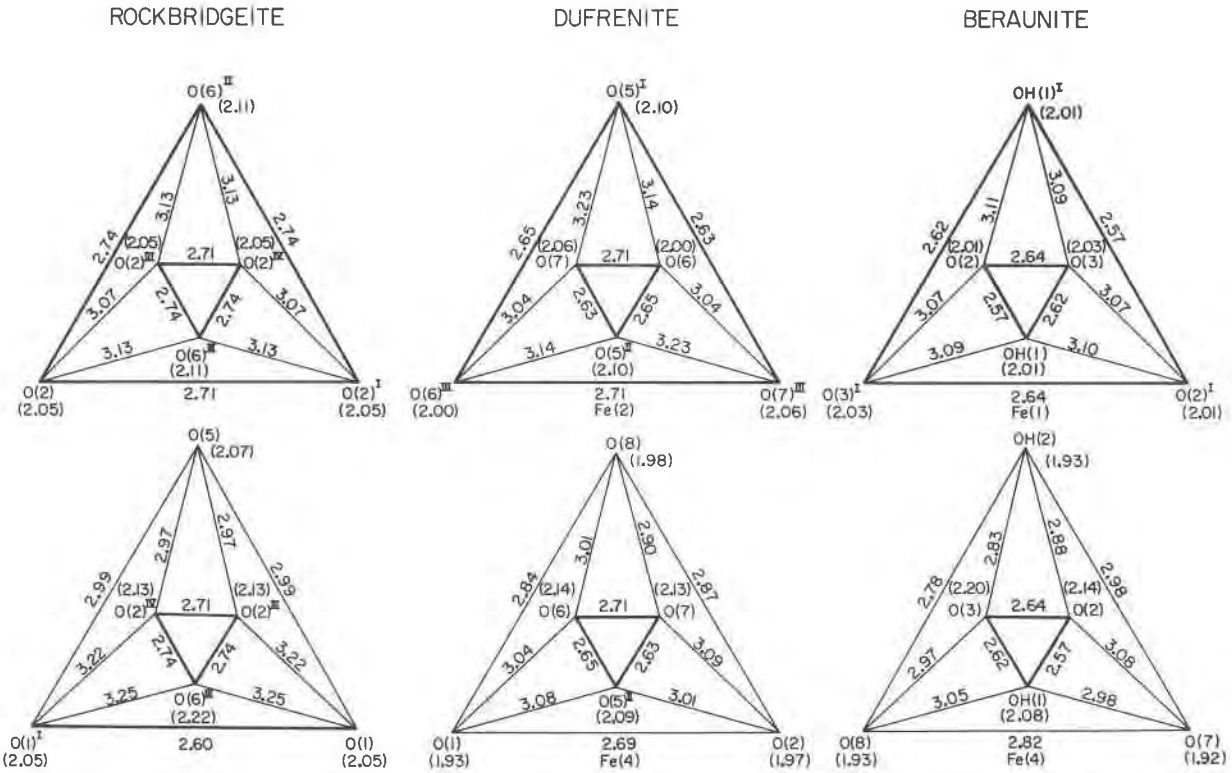

FIG. 4. Interatomic *M-O*, *T-O*, and *O-O'* distances in the rockbridgeite, dufrenite, and beraunite crystal structures depicted as the Schlegel diagrams of their polyhedra, arranged so that the Schlegel diagrams can be superimposed. Bold lines indicate shared edges. There is a one-to-one correspondence in position between the nodes, branches, and faces of the equivalent polyhedra in figures 1 and 2. The *M-O* and *T-O* distances are shown in parentheses, and the *O-O'* distances accompany their appropriate edges. Superscripts refer to symmetry equivalent atoms: in rockbridgeite, I=$x, y, \bar{z}$; II=$1/2+x, y, 1/2+z$, III=$\bar{x}, \bar{y}, z$; IV=$\bar{x}, \bar{y}, \bar{z}$; V=$1/2-x, \bar{y}, 1/2-z$; VI=$1/2+x, y, 1/2-z$; and VII=$x, 1/2-y, z$. In dufrenite, I=$1/2-x, 1/2+y, 1/2-z$; II=$x, \bar{y}, 1/2+z$; III=$1/2-x, 1/2-y, \bar{z}$; IV=$\bar{x}, \bar{y}, \bar{z}$; and V=$\bar{x}, y, 1/2-z$.

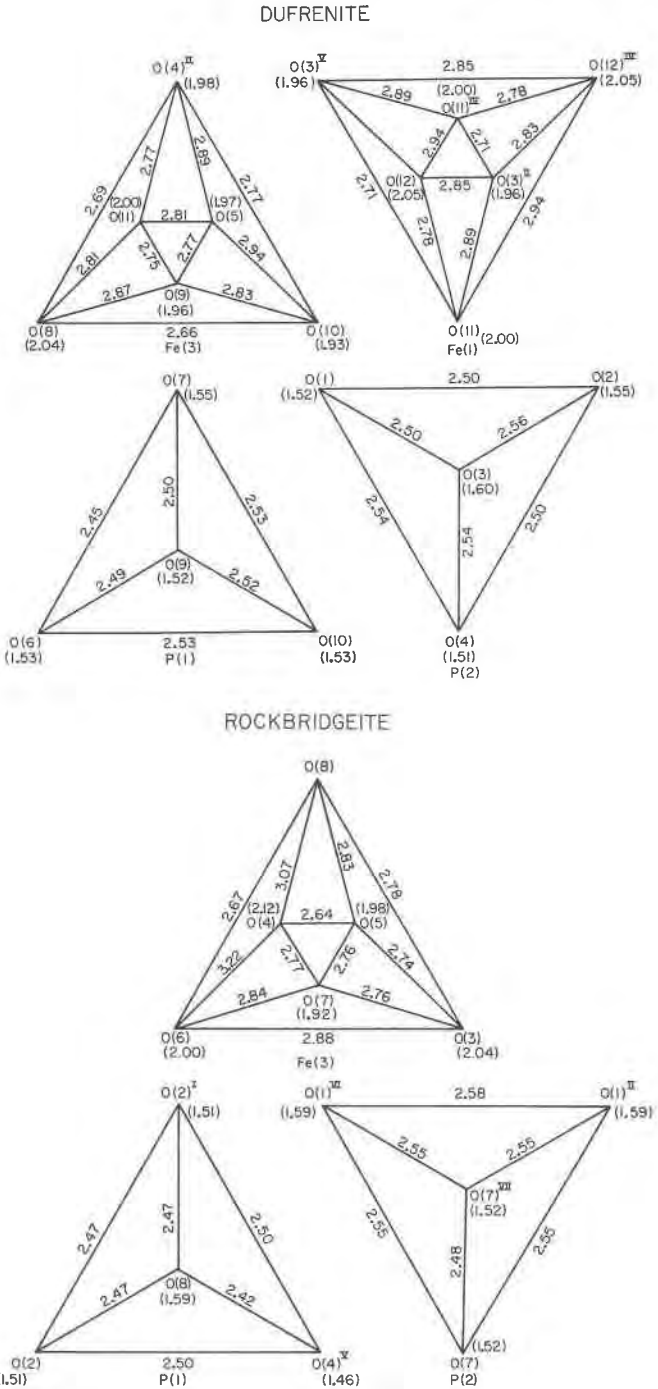

FIG. 5. Schlegel diagrams of the remaining nonequivalent octahedra and tetrahedra in (a) dufrenite and (b) rockbridgeite.

ing scheme. The resulting structure would be orthorhombic and, if centrosymmetric, have the space group *Pbmn*. Otherwise, the cell criteria would be similar to those for lipscombite.

Closely related is the barbosalite dimorph, isotypic to lazulite. Barbosalite, like the manganoan-lipscombite of Lindberg (1962), occurs as a late-stage hydrothermally reworked product of triphylite in pegmatites. Barbosalite is an ordered equivalent of the lipscombite structure, having isolated *h*-clusters instead of disordered face-sharing chains. It is not immediately obvious that the cell criteria for barbosalite in Table 2 are related to those of tetragonal lipscombite. If the triclinic pseudo-monoclinic cell with $a_t = a_m + 2c_m$; $b_t = a_m - b_m$; $c_t = a_m + b_m$ is chosen, its projection down c_t shows the relationship (Fig. 3b). The same dense slabs are found in this structure as in the others, but these slabs are linked laterally by the $(PO_4)^{3-}$ tetrahedra instead of bridging corner-sharing octahedral clusters. The coordinates of isotypic lazulite, determined by Lindberg and Christ (1959) were used for constructing this diagram.

The lipscombite-barbosalite dimorphism is further complicated by the allied mineral, manganoan-lipscombite. According to Lindberg (1962), the space group is not body-centered but primitive pseudobody-centered, *P*422 and the *a*-axis is related to that of lipscombite by the factor $\sqrt{2}$ (Table 2). Comparison of these data suggests that a family of ordered sequences may exist, ranging from the completely disordered lipscombite to the completely ordered barbosalite. The stability relationships of these sequences are unknown, and Gheith's (1953) study on the lipscombite-barbosalite pair is inconclusive for lack of detailed single crystal studies. Further work is necessary, before these compounds—particularly manganoan-lipscombite—can be precisely defined.

A yet larger polyatomic complex can be chosen common to the basic ferrous-ferric phosphate structures discussed above, if the nearest neighbor polyhedra around the *h*-cluster are considered. This includes the *h*-cluster and the four corner-linked nearest neighbor octahedra and their associated tetrahedra. The resulting packet of polyhedra, illustrated in Figure 6, is a convenient key to all the structures. As Table 2 shows, these compounds have one axis of *ca.* 13 Å length which, like the 5.1 Å fiber axis, appears to be invariant for these compounds.[1] The third crystal axis is variable and extends along the direction of the four short arrows in Figure 6. This figure also shows that the 13 and 5.1 Å axes lie in the plane of the dense slabs mentioned earlier and that the illustrated packet includes all the necessary ingredients for constructing these slabs. Alternatively stated, the variable axis is that axis along which the slabs are bridged together to form a three-dimensional arrangement.

[1] Choosing one-half the obtuse diagonal of *a* and *c* in beraunite yields 13.6 Å. This orientation conforms to the ca. 13 Å repeat in the other minerals.

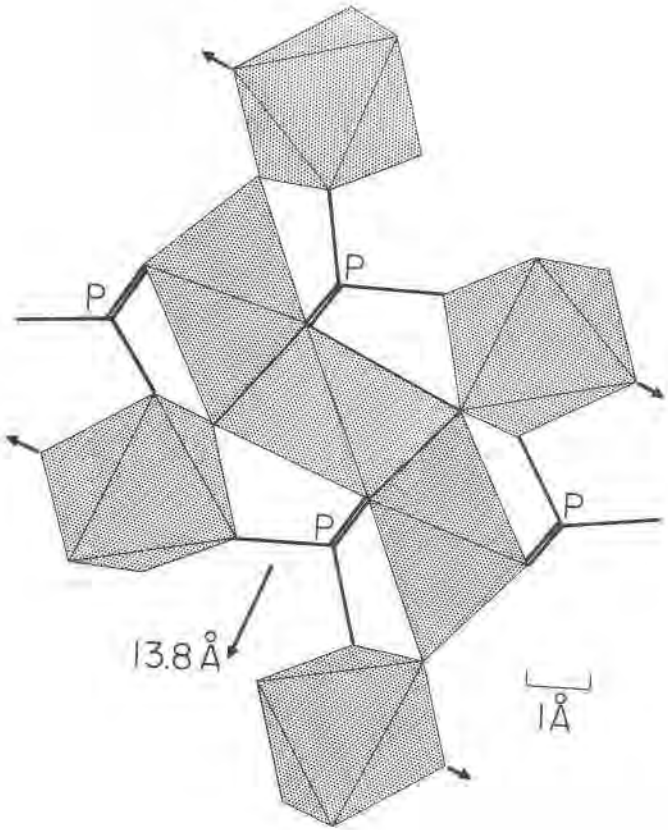

FIG. 6. The *h*-cluster and its immediate polyhedral neighborhood in the basic iron phosphates. The $(PO_4)^{3-}$ tetrahedra, shown as P-O spokes, share corners with the octahedra and are above and below the cluster. The axis normal to the plan of the diagram is the 5.1 Å fiber axis, and the 13.8 Å axis is the remaining "invariant" in these structures, these two directions in the plane of the polyhedral slabs. The remaining crystal axis, in the direction of the arrows, is variable.

Where do laubmannite and mineral A stand in relation to these arrangements? The cell criteria for these compounds leave little doubt that similar, if not identical principles also apply. Indeed, preliminary Patterson synthesis, $P(xy)$, for laubmannite conclusively confirms the presence of the *h*-cluster. However, the large number of atoms in the asymmetric unit, many of which lie outside the *h*-cluster and its immediate environment, poses a difficult problem for the structure analyst. Mineral A so far does not afford suitable single crystals for a parallel study, but it is apparently a variant of the laubmannite structure. Despite these impediments, I have derived plausible structures for these

minerals, but for lack of convincing experimental evidence, will not offer them here.

Pleochroism, Color and the h-*cluster*. One noteworthy feature of the basic iron phosphates in general is the dependence of color on valence states of the iron. Table 1 lists the iron phosphate hydrates and their typical colors. The ferrous compounds are pale-colored, in the greens and pinks and only weakly pleochroic. The ferric compounds are variously yellow, brown, red and pink and also only weakly pleochroic. However, the compounds involving both ferrous and ferric iron are extremely pleochroic and deep greenish-black in the gross sample. The colors in these compounds must result from effects distinct from the additive property of component colors of the pure ferrous and ferric salts. The oxidized ferric end-members of the ferrous-ferric phosphates are either orange, yellow or brown and only weakly pleochroic. Gheith documented the effect of valence on the color of lipscombite. Ferrous-ferric lipscombite is deep greenish-black and opaque except in the thinnest slices, whereas the ferric end-member is olive-yellow in color.

It is well-known that mixed valence states of a particular atomic species in the same crystal often contribute to dark colors. The problem involving mixed iron valences in minerals often falls into the realm of intervalence transfer absorption of the type involving symmetrical electron transfer between homonuclear cations (for an excellent review, see Allen and Hush, 1967). For such iron compounds, this can be written $Fe^{2+}+Fe^{3+}\rightleftharpoons Fe^{3+}+Fe^{2+}$. Absorption studies conducted by Hush (1967) on vivianite have led to the assignment of the band maximum of 15.1×10^3 cm^{-1} to $Fe^{2+}-Fe^{3+}$ intervalence transfer. This contribution is polarized parallel to the *b*-axis of the crystal which is the direction parallel to the axis including the two iron atoms separated by 2.95 Å in the octahedral doublet $Fe_2(H_2O)_4(O_p)_6$. This doublet corresponds to the edge-sharing *c*-cluster of Moore (1965). The mixed valences arise from partial oxidation of iron in the *c*-cluster, *viz.* $Fe^{2+}Fe^{3+}(OH)(H_2O)_3(O_p)_6$, resulting in the deep-blue color of the mineral corresponding to the vibration direction parallel to the *b*-axis. According to Hush, the ratio of Fe^{3+}/Fe^{2+} is about 0.05 for this crystal. In the basic iron phosphates, where such ratios are often much higher, the crystals can be very strongly absorbing to the extent of being nearly opaque except in the thinnest pieces. Since the probability of electron transfer and hence of absorption decreases with increasing interatomic distances, the short interatomic distance of *ca.* 2.7 Å between the metals in the *h*-cluster also renders electron transfer highly likely. The problem is not as simple as in the vivianite structure where the octahedral doublets are discrete and not interconnected by bridging Fe-centered oxygen octahedra. In the basic iron phosphates,

the *h*-cluster is further linked laterally by octahedra with Fe-Fe distances of *ca.* 3.5 Å. In rockbridgeite and lipscombite, the *h*-clusters are further fused by edge- and face-sharing respectively, forming chains with 2.7 Å and 3.2 Å Fe-Fe distances in the former, and partly occupied chains with Fe-Fe distances of 2.7 Å in the latter.

Small single crystals of greenish-black dufrenite, beraunite and rockbridgeite from the localities mentioned earlier were mounted on a spindle stage and oriented by X-rays so that spindle axis corresponded to the 5.1 Å fiber translation. These crystals were then examined on a polarizing petrographic microscope. Vibrations parallel to the fiber axis are least absorbed by the crystals and the pleochroism is pale orange-yellow with a slight greenish tinge. Vibrations perpendicular to the fiber axis are very strongly absorbed and the colors range from dark greenish-orange or red to deep blue or green. Figure 7 depicts the relationships of the pleochroic colors, the axial positions and the orientation of the *h*-cluster, projected down the fiber axis for dufrenite, beraunite and rockbridgeite.

It was first believed that the vibration direction with deep blue to green color would lie parallel to the axis of the *h*-cluster, analogous to the vibration direction of the blue pleochroic color in vivianite, corresponding to the axis of the double group in that mineral. The results show that the problem is far more complicated: in dufrenite and beraunite, the vibration direction with deep green color is oriented about 40 to 45° away from the axis of the *h*-cluster. In rockbridgeite, where the mirror planes yield two nonparallel *h*-cluster axes, the vibration directions coplanar to these axes range from bluish-green to dark bluish-green in color. These results indicate that the general problem of electron transfer absorption in crystals involving the *h*-cluster is very interesting, but will require much more elaborate analyses than the qualitative results offered here.

Paragenesis

Three important modes of occurrence are documented for the basic iron phosphates and include "limonite" and bog ore beds; hydrothermally reworked products in pegmatites; and replacements and cements in clays, sands and bone material.

The occurrence in "limonite" and bog ore beds is quite characteristic. Here, the minerals occur as fibrous encrustations and mammillary aggregates upon goethite, hematite, etc. Rockbridgeite from its type locality, for example, occurs as large blocks of fibrous masses associated with "limonite" beds. The mineral is also quite abundant in novaculite where ferric oxy-hydroxides have accumulated. Quite noteworthy are the many occurrences in prospect pits in the Ouachita Mountains, Arkansas. The

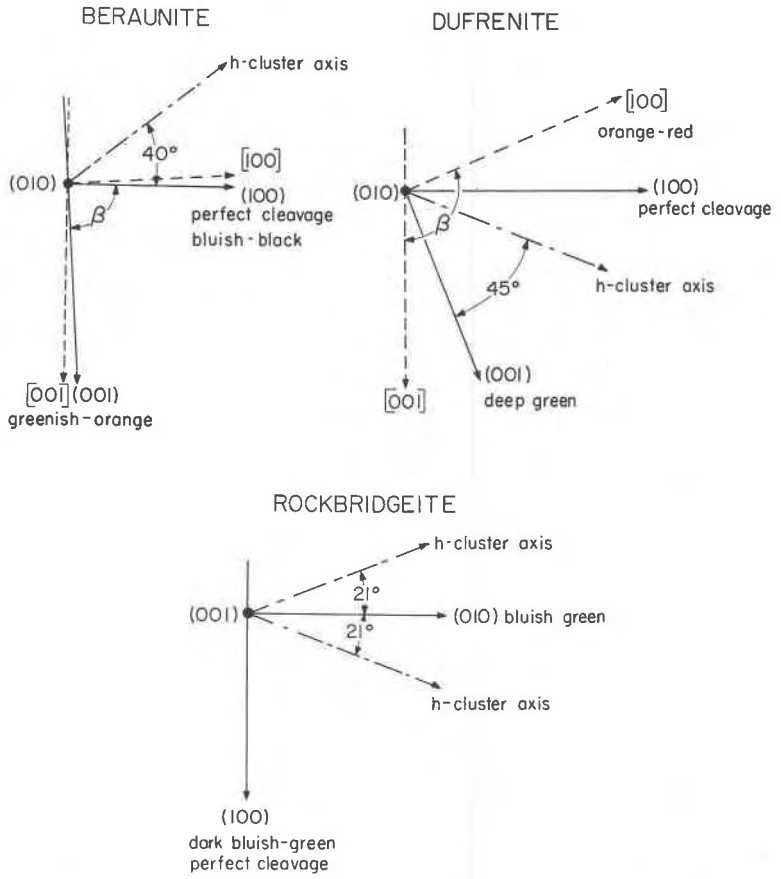

FIG. 7. Gnomograms showing the cleavage planes, crystal axes, *h*-cluster axes and absorption maxima for beraunite, dufrenite and rockbridgeite. The fiber axes are polar.

phosphates cap and replace botryoidal aggregates of goethite, and there is little doubt that the phosphates post-date the ferric oxy-hydroxides and probably represent products of ferric oxy-hydroxide reworking by phosphatic waters. The characteristic gum-like and botryoidal features of the surfaces and the appearance of shrinkage cracks indicate a gel origin or source for these minerals. Indeed, glassy patches of resinous deep-red material still remain, often showing partial to complete replacement by the iron phosphates. The powder patterns of some gels resemble goethite, and with broadened lines.

One locality, "Avant's Claim" near Shady, Polk Co., Arkansas, is a small nearly hidden pit showing bedded masses of porous goethite gel and dense botryoidal seams of the phosphates in brecciated novaculite.

The botryoids, when broken, show the characteristic radial aggregates of fibrils. The earliest phosphate to appear is greenish-black rockbridgeite, but it frequently grades outwardly into beraunite.

Another locality on Buckeye Mountain (near Shady) is the type locality for laubmannite. The mineral occurs as bright olive-green botryoidal and mammillary aggregates filling crevices in novaculite. In some instances, it replaces goethite. These laubmannites, when crystallized in open cavities, frequently terminate as brilliant deep emerald green crystals, which proved to be dufrenite on the basis of single crystal studies.

Both these localities clearly show less dense, more open hydrated structures replacing or following the earlier phases. This type of paragenesis indicates falling temperature to successive regions where the appearance of structures with increasing amounts of water molecules as ligands and as cavity fillers are rendered more stable. The general sequence is thus,

'dense' hydroxylated structures

$$\xrightarrow[+H_2O]{\text{lower T}} \text{open hydrated-hydroxylated structures.}$$

A remarkable occurrence at Fodderstack Mountain, Montgomery Co., Arkansas, shows fibrous masses of rockbridgeite with mammillary surfaces and color banding. Rockbridgeites frequently show color bands at millimeter intervals, involving the colors black, yellow, orange and blue. In open cavities, the rockbridgeite is frequently postdated by a vivid yellowish-green material. Through careful dissection of fibers showing color banding, sphere mount powder patterns were prepared. The color bands proved to result from the appearance of different phases, with black = rockbridgeite, yellow-orange = yellowish-green = mineral A, and blue = lipscombite. The powder data for lipscombite in these specimens appear in Table 3. X-ray study of a large rockbridgeite from Rockbridge Co., Virginia, capped by the yellow pulverulent product described by Frondel (1949) shows that the latter material is a mixture of mineral A + goethite. Finally, I would like to point out the similarity of Frondel's powder pattern of an unknown phosphate from Waldgirmes, Saxony with mineral A (Table 3). Mineral A appears to be a fairly typical product of rockbridgeite leaching. The rhythmic color banding in the Fodderstack materials indicates a mode of origin somewhat different than the earlier mentioned parageneses. Perhaps these phases crystallized from a gel with rhythmic alternations of $FeO:Fe_2O_3:P_2O_5:H_2O$ ratios or through rhythmic fluctuations in pH.

Rockbridgeite is a rather abundant hydrothermally reworked product

of triphylite in granite pegmatites and specimen study shows the mineral in a range of associations and sequences, usually appearing earlier than the other minerals. Only a few specimens could be located which showed rockbridgeite partly replaced by another mineral. Several specimens from Palermo #1 in the Bjareby collection show rockbridgeite fibers replaced near the surface by orange beraunite. Another specimen shows rockbridgeite fibers tipped with olive-green dufrenite. These observations parallel the settings observed in the Arkansas materials. The counter example—showing the more open structures replaced by denser ones—has not been observed.

It is proposed that the typical sequence of replacement and/or paragenetic succession in the basic iron phosphates is

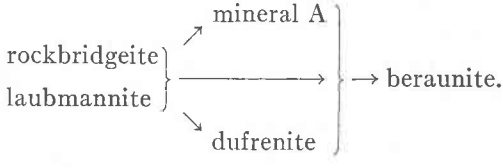

Further Remarks

Despite the increase in the number of investigations on the basic phosphates of iron, our knowledge of the group is still incomplete. Of the list of 40 species in Table 1, the atomic arrangements are known for only 15 of them. If the aluminum- and calcium-rich iron phosphates are added to the list, the number of species increases considerably, for which only a few atomic arrangements are known.

Some of the more incompletely understood iron phosphates may prove to be related to the family involving the *h*-cluster described in this paper. Cacoxenite, for example, is an intriguing substance. A superior single crystal of this mineral from Shady, Arkansas, was secured from the Bjareby collection and yielded the data in Table 2. For crystal-chemical calculations, I used the analysis of Church (1895), which is probably more reliable than the other analyses reported for the mineral. Assuming the water removed by desiccation over sulfuric acid is zeolitic, the formula is close to $Fe_9(OH)_{15}(H_2O)_3(PO_4)_4 \cdot 15H_2O$. Halving the *a*- and *c*-axes yield 13.80 and 5.22 Å respectively, similar to the "invariants" for the structures discussed herein. The cavities in this structure are probably quite large and the arrangement may be similar to that of the zemannite structure, discussed by Matzat (1966). Zemannite is a hexagonal tellurite mineral with large 8 Å in diameter channels filled by water molecules and alkalis. Indeed, guided by the cell criteria, *h*-clusters can be linked to form an open honeycomb structure, and this model is presently being tested.

Another group includes the gel-like basic calcian ferric phosphates eguëite, richellite, azovskite (in part), mitridatite (in part), borickyite and foucherite. Many of these are chemically closely related if not identical to each other. Their compositions are reminiscent of the dufrenite formula. Do these gels contain disordered *h*-clusters? Interesting in this aspect is the experiment of McConnell (1963), where thermal recrystallization of richellite was shown to produce a calcium variant of the lipscombite structure. If this recrystallization is assumed to follow a mechanism akin to the recrystallization of metamict materials, then the *h*-clusters were probably present in the gel state, suggesting that these amorphous minerals formed in an environment similar to the crystalline basic ferrous-ferric phosphate minerals. These gel materials may be remnants of the early-formed liquors from which the crystalline ferrous-ferric phosphates grow.

ACKNOWLEDGMENTS

Specimens of basic iron phosphates, many of which were sacrificed for study, were donated by Messrs. J. K. Nelson and A. Kidwell, and Prof. J. V. Smith. Dr. J. J. Fahey arranged for me to obtain crystals of type souzalite, housed in the U.S. National Museum and donated by Dr. G. Switzer. Mr. S. J. Louisnathan assisted in the computation of the powder data and Mr. C. Stern in the intensity collection for dufrenite. Prof. D. R. Peacor kindly read the manuscript and offered helpful suggestions as to its improvement.

This work was made possible through the NSF grant GA-907 and an ARPA grant administered to the Department of the Geophysical Sciences.

REFERENCES

ALLEN, G. C., AND N. S. HUSH (1967) Intervalence-transfer absorption. 1. *Prog. Inorg. Chem.* **8,** 357–386.

CAMPBELL, J. L. (1881) On dufrenite from Rockbridge County, Va. *Amer. J. Sci.* **22,** 65–67.

CHURCH, A. H. (1895) A chemical study of some native arsenates and phosphates. 6. Cacoxenite. *Mineral. Mag.* **11,** 8–10.

CLARINGBULL, G. F., AND M. H. HEY (1958) A re-examination of andrewsite. *Mineral. Soc. Notice* **100,** 1.

COXETER, H. S. M. (1947) *Regular Polytopes.* Pitman Publishing Corp., New York, p. 10.

FANFANI, L. AND P. F. ZANAZZI (1967) The crystal structure of beraunite. *Acta Crystallogr.* **22,** 173–181.

FRONDEL, C. (1949) The dufrenite problem. *Amer. Mineral.* **34,** 513–540.

GHEITH, M. A. (1953) Lipscombite, a new synthetic "iron lazulite." *Amer. Mineral.* **38,** 612–627.

HUSH, N. S. (1967) Intervalence-transfer absorption. 2. *Prog. Inorg. Chem.* **8,** 401–405.

KATZ, L. AND W. N. LIPSCOMB (1951) The crystal structure of iron lazulite, a synthetic mineral related to lazulite. *Acta Crystallogr,* **4,** 345–348.

KINCH, E. AND F. H. BUTLER (1886) On a new variety of mineral from Cornwall. *Mineral. Mag.* **7,** 65–70.

LINDBERG, M. L. (1949) Frondelite and the frondelite-rockbridgeite series. *Amer. Mineral.* **34,** 541–549.

——— (1962) Manganoan lipscombite from the Sapucaia Pegmatite Mine, Minas Gerais, Brazil. *Amer. Mineral.* **47** 353–359.

———, AND C. L. CHRIST (1959) Crystal structures of the isostructural minerals lazulite, scorzalite and barbosalite. *Acta Crystallogr.* **12,** 695–696.

MATZAT, E. (1966) Die Kristallstruktur eines unbekannter zeolithartigen Tellurit-minerals. *Tschermaks Mineral. Petrograph. Mitt.* **12,** 108–117.

MCCONNELL, D. (1963) Thermocrystallization of richellite to produce a lazulite structure (calcium lipscombite). *Amer. Mineral.* **48,** 300–307.

MOORE, P. B. (1965a) A structural classification of Fe-Mn orthophosphate hydrates. *Amer. Mineral.* **50,** 2052–2062.

——— (1965b) The crystal structure of laueite. *Amer. Mineral.* **50,** 1884–1892.

——— (1969) The basic ferric phosphates: a crystallochemical principle. *Science,* **164,** 1063–1064.

MROSE, M. E. (1955) Problems of the iron-manganese phosphates (abstr.). *Geol. Soc. Amer. Bull.* **66,** 1660.

PALACHE, C., H. BERMAN AND C. FRONDEL (1951) *The System of Mineralogy . . . of Dana. Vol. 2.* John Wiley and Sons, New York, p. 960.

PECORA, W. T. AND J. J. FAHEY (1949) The Corrego Frio Pegmatite, Minas Gerais: scorzalite and souzalite, two new phosphate minerals. *Amer. Mineral.* **34,** 83–93.

Manuscript received May 29, 1969; accepted for publication September 20, 1969